Hydrodynamic and Functional Analysis of HIV-1 Vif Oligomerization

ARTICLE *in* BIOCHEMISTRY · MARCH 2012

Impact Factor: 3.02 · DOI: 10.1021/bi201738a · Source: PubMed

Published in final edited form as:
Biochemistry. 2012 March 13; 51(10): 2078–2086. doi:10.1021/bi201738a.

Hydrodynamic and Functional Analysis of HIV-1 Vif Oligomerization

Stephen M. Techtmann[1], **Rodolfo Ghirlando**[2], **Sandra Kao**[3], **Klaus Strebel**[3], and **Ernest L. Maynard**[1,*]

[1]Department of Biochemistry and Molecular Biology, USUHS

[2]Laboratory of Molecular Biology, National Institute of Diabetes, Digestive and Kidney Diseases, National Institutes of Health, Bethesda MD 20892

[3]Laboratory of Molecular Microbiology, National Institute of Allergy and Infectious Diseases, National Institutes of Health, Bethesda MD 20892

Abstract

HIV-1 Vif is an accessory protein that induces the proteasomal degradation of the host restriction factor, apolipoprotein B mRNA-editing enzyme catalytic polypeptide-like 3G (APOBEC3G). The N-terminal half of Vif binds to APOBEC3G and the C-terminal half binds to subunits of a cullin-5-based ubiquitin ligase. This Vif-directed ubiquitin ligase induces the degradation of APOBEC3G (a cytidine deaminase), and thereby protects the viral genome from mutation. A conserved PPLP motif near the C terminus of Vif is essential for Vif function and is also involved in Vif oligomerization. However, the mechanism and functional significance of Vif oligomerization is unclear. We employed analytical ultracentrifugation to examine the oligomeric properties of Vif in solution. Contrary to previous reports, we find that Vif oligomerization does not require the conserved PPLP motif. Instead, our data suggest a more complex mechanism involving interactions between the HCCH motif, BC box, and downstream residues in Vif. Mutation of residues near the PPLP motif (S165 and V166) affected the oligomeric properties of Vif and reduced the ability of Vif to bind and induce the degradation of APOBEC3G. We propose that Vif oligomerization may represent a mechanism to regulate interactions with APOBEC3G.

HIV-1 virion infectivity factor (Vif)* is an accessory protein that is required for viral replication in T cells. Such “non-permissive” cells restrict the replication of *vif*-deficient HIV-1 because they express apolipoprotein B mRNA-editing enzyme catalytic polypeptide-like 3G (APOBEC3G) (1) as well as the closely related APOBEC3F (2–5). APOBEC3G contains two copies of the cytidine deaminase (CDA) domain. The N-terminal CDA domain mediates packaging of APOBEC3G into virus particles (6) by a process that involves interactions with the nucleocapsid domain of Gag (6–15). APOBEC3G is delivered in the virus particle to the target cell where it catalyzes the deamination of cytidines in the minus strand DNA produced by viral reverse transcription. The resulting C-to-U mutations are copied into the plus strand DNA as G-to-A mutations that block viral replication (2–5, 16–20). Vif prevents the encapsidation of APOBEC3G into virus particles. Vif functions as an

*Corresponding author emaynard@usuhs.mil Tel: 301-295-2845; Fax: 301-295-3512.

Supporting Information Available Size-exclusion analysis of MBP-Vif(154–176) and supporting sedimentation velocity data for MBP-Vif(101–176). This material is available free of charge via the Internet at http://pubs.acs.org.

Conflict of Interest Disclosure The authors declare no competing financial interest.

*Abbreviations: APOBEC3G, apolipoprotein B mRNA-editing enzyme catalytic polypeptide-like 3G; AUC, analytical ultracentrifugation; CD, circular dichroism; PPLP peptide, Vif residues 155–176; RING, really interesting new gene; SOCS, suppressor of cytokine signaling; Vif, virion infectivity factor

adaptor protein that binds to APOBEC3G and to subunits of a RING-cullin ubiquitin ligase, including elongin B/C and cullin 5 (Cul5) (21). This complex, which includes the recently identified T-cell differentiation factor CBF-β (22, 23), induces the polyubiquitination and proteasomal degradation of APOBEC3G (21, 24–28).

HIV-1 Vif is a 23-kDa protein of 192 amino acids. APOBEC3G binds to a surface in Vif formed by a non-linear array of sequence motifs that span residues 14–89 (29–35). Elongin B/C binds to the conserved BC box motif in Vif (S^{144}LQYLALAAL^{153}) (36, 37). Two regions in Vif appear to be important for binding to Cul5. The HCCH motif ($H^{108}C^{114}C^{133}H^{139}$) is required for interaction with Cul5 (38–41). Zinc binds specifically and reversibly to the HCCH motif to generate a conformation capable of mediating protein-protein interactions (42). An HCCH-containing fragment of Vif (residues 101–141) interacts directly with Cul5 in a zinc-dependent manner, suggesting that zinc modulates the conformation of Vif to expose a Cul5 binding site (41). The $P^{161}PLP^{164}$ motif located downstream from the BC box has also been implicated in Cul5 binding (43, 44), and bears sequence similarity to the Cullin box motif that is conserved in suppressor of cytokine signaling (SOCS) proteins (45). However, the PPLP motif appears to play a minor thermodynamic role in forming the Vif-Cul5-elongin BC complex, which is driven by the high (nanomolar) affinity of the BC box for elongin B/C (44). A recent NMR study demonstrated that the PPLP motif binds to elongin B (46) and other studies suggest that the PPLP motif is required for APOBEC3G binding and degradation (47, 48). The PPLP motif is located in a region of Vif that is highly dynamic in solution (49, 50). Flexibility may allow this region of Vif to engage in diverse protein-protein interactions.

The ability of Vif to form diverse protein-protein interactions is further exemplified by the discovery that Vif forms homo-oligomers. Using a pull-down assay with GST-Vif and ^{35}S-labeled Vif, the region in HIV-1 Vif required for oligomerization was mapped to residues 151–164, which contains the conserved $P^{161}PLP^{164}$ motif (51). Deletion of the PPLP motif inhibited the interaction between GST-Vif and ^{35}S-Vif, and peptides containing the PPLP motif suppressed viral infectivity, suggesting that the PPLP motif is essential for oligomerization and function of HIV-1 Vif (52). Virus particles produced from cells treated with peptide antagonists of HIV-1 Vif oligomerization contained elevated amounts of APOBEC3G, further suggesting that oligomerization is critical for Vif function (53). Despite the progress that has been made, a clear mechanistic understanding of Vif oligomerization is lacking. Towards this goal, we have employed analytical ultracentrifugation (AUC) to examine the oligomeric properties of Vif. These studies are complemented by functional assays to gauge the impact of mutations that affect the oligomeric state of Vif on the ability to bind to and induce the degradation of APOBEC3G.

Materials and Methods

Cloning, Protein Expression, and Purification

Vif fragments were cloned into the pMal c-5x vector (NEB) using EcoRI and SbfI sites. Site-directed mutagenesis was performed using the QuikChange II XL mutagenesis kit (Agilent Technologies). Constructs were transformed into BL21 (DE3) *Escherichia coli* cells. Bacteria were cultured in 2YT broth containing ampicillin and 1% glucose at 37°C until OD_{600} = 0.6. Protein expression was induced with 0.5 mM IPTG and allowed to occur for 16 hr at 18°C. Cells were harvested by centrifugation at 5,500 × *g* at 4°C.

Cells were resuspended in Buffer A (20 mM HEPES pH 7.5, 150 mM NaCl, 200 μM TCEP) supplemented with RNase/DNase and protease inhibitor (Roche Applied Sciences) and lysed in a French pressure cell. Lysates were clarified by centrifugation at 18,000 × *g* at 4°C for 30 minutes. The supernatant was allowed to incubate with amylose resin for 1 hr at 4°C

and the resin was washed with five column volumes of Buffer A, followed by five column volumes of Buffer B (20 mM HEPES pH 8.0, 20 mM NaCl, 200 μM TCEP). Proteins were eluted with two column volumes of buffer B plus 10 mM maltose. Vif-containing fractions were loaded onto a Resource Q column (GE Healthcare) equilibrated with Buffer B. After washing with Buffer B the protein was eluted by a linear gradient from 20 mM NaCl to 1 M NaCl over 10 column volumes. Vif was further purified by a Superose 6 column equilibrated in Buffer A and at a flow rate of 0.5 mL min^{-1}. Protein concentration was determined by either Bradford assay (Bio-Rad) using bovine serum albumin as a standard or by the method of Edelhoch as described in Pace *et al* (54).

Analytical Ultracentrifugation

Sedimentation velocity experiments were conducted at 20.0°C on a Beckman Coulter Proteome XL-A or XL-I analytical ultracentrifuge using the absorbance optical detection system. Samples were loaded into 2-channel, 12 mm path length sector shaped cells (400 μL). Scans were acquired at 4 minute intervals and rotor speeds of 45,000 rpm; absorbance data were collected as single absorbance measurements at either 280 or 250 nm using a radial spacing of 0.003 cm.

Data were analyzed in SEDFIT 11.9b (55) in terms of a continuous c(*s*) distribution. Solution densities ρ and viscosities η were calculated using the program SEDNTERP 1.2 (56), as were values for the partial specific volume *v* of the protein. The c(*s*) analyses were carried out using an *s* range of 0 to 25 with a linear resolution of 200 and maximum entropy regularization confidence levels (F-ratio) of 0.68. In all cases, excellent fits were observed with root mean square deviations ranging from 0.0030 – 0.0091 absorbance units. Sedimentation coefficients were corrected to standard conditions at 20.0°C in water, $s_{20,w}$. Weighted-average sedimentation coefficients, combining contributions from the monomer and oligomer, were obtained from the integral of the c(*s*) distributions. These were used to construct weighted average sedimentation coefficient isotherms for the absorbance data.

Vif(155–176) (PPLP peptide) preparation and analysis by CD spectroscopy

HIV-1 Vif residues 155–176 (TPKKIKPPLPSVTKLTEDRWNK) was synthesized by solid phase peptide synthesis using Fmoc protection (Peptide 2.0, Chantilly VA.). Crude peptides were solubilized and purified by reversed phase HPLC as previously described (42). The peptide was dissolved in Buffer A and concentrations were determined using the method of Edelhoch as described in Pace *et al* (54).

Peptide samples for far-UV CD spectroscopy were diluted to 48 μM in 10 mM MOPS pH 7.4, 20 mM NaCl, and 40 μM TCEP. Solutions were placed in quartz cuvettes with path lengths of 1 mm and far-UV CD spectra were recorded using a JASCO J-815 spectrometer at a scan speed of 20 nm/min and a bandwidth of 1 nm. Each spectrum represents the average of five successive baseline-corrected scans. Sample temperature for all CD measurements was maintained at 20°C.

The mean residue molar ellipticity, [θ], was calculated according to the equation, $[\theta] = (\theta \cdot MR)/(10 \cdot l \cdot c)$. θ is the measured ellipticity in millidegrees, MR is the mean residue mass (molecular weight of the peptide divided by the number of amino acid residues), *l* is the optical path length in cm and *c* is the protein concentration in mg/mL. Spectral deconvolution was performed using the Contin algorithm (57) using the reference set SP175 (58) from the suite of programs available at the online server DICHROWEB (www.cryst.bbk.ac.uk/cdweb) (59, 60).

APOBEC3G degradation Assay

HeLa cells were transfected with pcDNA-APOBEC3G (0.5 μg) and pNL-A1-Vif constructs (4.5 μg). Cells were harvested 24 hr later and whole cell lysates were subjected to immunoblotting using antibodies to APOBEC3G or Vif. The APOBEC3G blot was subsequently reprobed with an antibody to tubulin, which served as a loading control.

Vif-APOBEC3G co-immunoprecipitation

HeLa cells were transfected with pcDNA-APOBEC3G-Myc (2 μg), pNL-A1-Vif (2 μg), and dominant negative Cul5 (21) (Cul5ΔRbx; 1 μg). Cul5ΔRbx was included to prevent Vif-induced A3G degradation in this experiment. Cells were harvested 24 hr later, lysed in CHAPS/DOC lysis buffer, and immunoprecipitated with a Myc-specific polyclonal antibody. Immunoprecipitates were separated by SDS-PAGE and probed with monoclonal antibodies to Vif and Myc. Amounts of wt Vif were defined as 100%. Amounts of co-precipitated mutant Vif proteins are expressed as percentage of wt Vif. Vif values were corrected for fluctuations in the APOBEC3G pull-down.

Results

Full-length Vif is prone to aggregation (42) and previous studies have indicated that the Vif C-terminal PPLP motif is responsible for oligomerization (51, 61). To avoid complications involving the Vif N-terminal domain (Vif residues 1–100), a domain that has a high affinity for nucleic acids (62, 63), we chose to focus on Vif C-terminal fragments (Vif residues 101−*x*). Several truncations were made in the Vif C terminus to highlight the regions involved in oligomerization and to assess the importance of the PPLP motif in oligomerization (Fig. 1a). Vif fragments were expressed and purified as fusions to maltose-binding protein (MBP). MBP fusion results in high levels of expression in *E. coli*, facilitates rapid protein purification, and MBP is monomeric in solution. Fig. 1b demonstrates the purity of the MBP fusion constructs used in this study.

Sedimentation c(*s*) profiles for MBP-Vif(101–192), MBP-Vif(101–176), and MBP, presented in Fig. 2, reveal that the MBP-Vif fragments are highly oligomeric and that MBP is almost completely monomeric. The c(*s*) plot for MBP did reveal a small peak at 5.8 S, consistent with dimer, accounting for ~10% of total protein. MBP used in this study contained the vector-derived sequence NAAAEFPAGN, which could promote non-specific dimerization. In support of this, when MBP was cloned and expressed without these additional amino acids, AUC revealed that the protein is monomeric at high concentrations (64). The species observed around $s_{20,w}$ = 3.8 S (44 kDa) have estimated molecular masses in close agreement with the calculated molecular masses of the monomeric MBP-Vif(101–176) (50 kDa) and MBP-Vif(101–192) (52 kDa). We note that the c(*s*) analysis involves direct boundary modeling of the sedimentation velocity data in terms of a distribution of Lamm equation solutions. In order to account for boundary broadening due to diffusion, the analysis assumes that all of the sedimenting particles in the distribution have the same frictional ratio f/f_o which may not necessarily be the case. This value, used to relate the sedimentation coefficient and molecular mass, is predominantly determined by the major species.

The c(*s*) profiles were integrated from 2.0–20.0 S to determine the fraction of protein present as monomer. This analysis revealed that, at the standard loading concentration of 10 μM, less than 30% of MBP-Vif(101–176) and MBP-Vif(101–192) were present as monomers. To address the reversibility of Vif oligomerization, the fraction of monomeric MBP-Vif(101–176) was measured as a function of protein concentration. A stock solution of 46.5 M MBP-Vif(101–176) was serially diluted and analyzed by sedimentation velocity

AUC. The percent of monomeric species was determined by integrating the c(*s*) profiles and is plotted as a function of protein concentration in the inset to Fig. 2. The data show a precipitous drop in monomer content from 42% to 10% as the protein concentration was increased from 1 μM to 15 μM. Beyond 15 μM, there was little change in the percent of monomer. Consistent with the percent monomer data, the weighted-average $s_{20,w}$ value, obtained by integrating the sedimentation c(*s*) profile from 2.0 – 20.0 S, increased with increasing protein concentration (data not shown). Due to the limits of detection provided by the absorbance and interference optics, we were unable to analyze protein samples at concentrations of less than 1 μM. However, even at 1 μM a large fraction of Vif (58%) was still oligomeric. Overall, the data in the inset to Fig. 2 demonstrate the reversibility of Vif oligomerization and illustrate the strong dependence on protein concentration.

Data presented in Fig. 2 suggest that the last 16 residues in Vif (177–192) are not required for oligomerization. The MBP-Vif(101–176) fragment contains the HCCH motif, BC box, and PPLP motif. Since previous studies have focused on the PPLP motif as being essential for Vif oligomerization, we studied the oligomeric properties of MBP-Vif(154–176), which contains the PPLP motif, but lacks both the HCCH motif and BC box. The c(*s*) profile for MBP-Vif(154–176) (Fig. 3) revealed that the protein was predominantly monomeric (>90% with $s_{20,w}$ = 3.7 S) with a small but significant amount of dimeric species ($s_{20,w}$ = 5.4 S). Due to the size of MBP, we wondered if the fusion tag could sterically hinder Vif oligomerization. A tag-free “PPLP peptide” (Vif residues 155–176), synthesized by solid-phase peptide synthesis and purified by reversed-phase HPLC, was therefore analyzed by sedimentation velocity AUC. At concentrations as high as 1.8 mM, the PPLP peptide sedimented as a single species with an $s_{20,w}$ = 0.45 S (Fig. 3) and best-fit molecular mass of 2,690 Da, which is (within the error of the method) identical to that calculated for the peptide monomer (2,577 Da). As the value of the sedimentation coefficient does not change over the 10-fold concentration range studied, the data in Fig. 3 strongly suggest that the PPLP peptide does not oligomerize. The data indicate that the PPLP motif alone is not sufficient to promote oligomerization of Vif and suggest the possibility that interaction with other upstream sequences (*e.g.* the BC box and HCCH motif) is required for oligomerization.

A small but significant amount of MBP-Vif(154–176) was dimeric (see the 5.4-S peak in Fig. 3). MBP and MBP-Vif(154–176) were also analyzed by size exclusion chromatography. MBP eluted from the column as a narrow peak consistent with the monomer while MBPVif(154–176) eluted in a broader peak indicating the presence of higher molecular-weight species in addition to the major monomeric species (Supplemental Data, Fig. S1). It is possible that MBP induces a conformational change in the PPLP peptide that facilitates dimerization. The far-UV CD spectrum of the PPLP peptide revealed that it is largely unstructured in solution (Fig. 4). Trifluoroethanol (TFE), a solvent well known for its ability to induce structure in peptides and proteins (65), was used to determine whether structural changes in the PPLP peptide could affect its oligomeric properties. Addition of TFE (20% or 40% v/v) to the PPLP peptide altered the far-UV CD spectrum, indicating a change in secondary structure (Fig. 4). Data analysis revealed that the percentage of alpha-helical secondary structure in the PPLP peptide increased from 5% in buffer lacking TFE to 15% in a solution containing 40% TFE. Sedimentation velocity AUC experiments revealed that TFE induced oligomerization of the PPLP peptide (Fig. 4, inset). The c(*s*) profiles of the PPLP peptide prepared in increasing concentrations of TFE illustrate a clear trend from a monomeric form (0.45 S) in the absence of TFE to a higher molecular-weight form (0.75 S) in the presence of 40% TFE. As sedimentation velocity AUC data interpretation depends critically on solvent densities and viscosities, the $s_{20,w}$ values were corrected for the changes in solution viscosity and density caused by TFE using SEDNTERP. Ignoring possible contributions from hydration terms to the buoyant molecular mass and using a peptide

partial specific volume calculated in SEDNTERP, we determine a best-fit molecular mass of 5,210 Da for the 0.75 S species in 40% (v/v) TFE, consistent with a peptide dimer (M_{calc} = 5,154 Da). As corrections for hydration contributions will only lead to larger true molecular masses, we conclude that the addition of TFE to the PPLP peptide induced a transition from a monomer to an oligomer (most likely dimer), suggesting that a modest change in the conformation of Vif residues 155–176 can promote oligomerization.

To identify other regions in the Vif C terminus required for oligomerization, we analyzed MBP-Vif (101− *x*) fragments (where *x* = 141, 153, 160, 165, or 172) by sedimentation velocity AUC. The c(*s*) profiles for MBP-Vif(101–141) and MBP-Vif(101–153) revealed major sedimenting species with $s_{20,w}$ = 3.6 S and 3.8 S, respectively (Fig. 5). Molecular masses for these species, corresponding to 42.7 kDa and 43.6 kDa, indicate that these represent monomeric MBP-Vif(101–141) (M_{calc} = 46.1 kDa) and MBP-Vif(101–153) (M_{calc} = 47.3 kDa), respectively. In addition to the dominant monomeric species, oligomers of MBP-Vif(101–141) and MBPVif(101–153) were also observed (Fig. 5). However, the extent of oligomerization observed for the Vif(101–141) and Vif(101–153) fragments was far less than what was observed for the Vif(101–176) fragment. Integration of the c(*s*) profiles for the Vif(101–141) and Vif(101–153) fragments revealed that these proteins are about 60% monomeric compared to the Vif(101–176) fragment which is 30% monomeric at the same loading concentration. Vif fragments longer than 101–153 (101–160, 101–165, and 101–172) were mostly oligomeric, forming a distribution of species ranging from $s_{20,w}$ = 5–20 S (Fig. 5). In these cases, less than 30% of the protein was monomeric, comparable to the Vif(101–176) fragment.

The weighted-average $s_{20,w}$ value, obtained by integrating the c(*s*) profile from 2.0 – 20.0 S, was calculated for each MBP-Vif construct (filled bars in the inset to Fig. 5). This value was compared to the monomer $s_{20,w}$ value for each construct (empty bars). The monomer $s_{20,w}$ values increase as expected for the changes in the size of the Vif fragments. Comparison of the weighted-average $s_{20,w}$ values reveals that the most significant increase in oligomeric species was due to residues 154–160 (compare the weighted-average $s_{20,w}$ values for the 101–153 and 101–160 fragments of Vif). Addition of residues 161–165 which encompass the PPLP motif did not cause an increase in the weighted-average $s_{20,w}$ value, further emphasizing the fact that the PPLP motif is not essential for Vif oligomerization.

Mutations were engineered into and surrounding the PPLP motif in MBP-Vif(101–176) and the effects on oligomerization were determined by sedimentation velocity AUC. We mutated the PPLP motif to AALA in the backbone of the MBP-Vif(101–176) construct to determine the role of the conserved proline residues in oligomerization. Inspection of the c(*s*) profile for MBPVif(101–176)$_{AALA}$ revealed that this mutant contained much less of the monomeric form and more oligomers than the wild type construct (Fig. 6a). Two other PPLP mutants were analyzed, namely PPLP → PPGP (L163G) and PPLP → PPPP (L163P). MBP-Vif(101–176)$_{PPGP}$ and MBP-Vif(101–176)$_{PPPP}$, also formed oligomers (Fig. 6a), demonstrating that mutation of the PPLP motif does not abolish oligomerization. The data support the idea that the PPLP motif is not required for oligomerization. Instead the PPLP motif may orient surrounding residues that make contacts in the oligomer.

Two highly conserved residues near the PPLP motif, V166 and S165, were mutated in MBP-Vif(101–176) to determine their role in Vif oligomerization. Mutation of V166 to S caused a dramatic reduction in monomer and an increase in the amount of dimer (Fig. 6b). This effect can be seen in the monomeric region of the c(*s*) profiles ($s_{20,w}$ = 3.6 – 4 S) where the amount of monomer detected for the V166S mutant was significantly less than in wild type Vif. In addition, the $s_{20,w}$ peak at 6 S (corresponding to dimer) was much more pronounced for the V166S mutant. Comparison of the c(*s*) profiles for the S165D and

S165A mutants revealed that these mutations stabilized the monomeric form of MBP-Vif(101–176) (Fig. 6b). This effect can be seen in the monomeric region of the c(*s*) profiles ($s_{20,w}$ = 3.6 – 4 S). The increase in monomeric species for the S165D and S165A mutants was balanced by a decrease in the amount of oligomers ($s_{20,w}$ = 7.0 – 15 S). Notably, the amount of dimer ($s_{20,w}$ = 6 S) was very similar between wild type Vif and the S165 mutants (Fig. 6b).

The V166S, S165D, and S165A mutations were generated in full-length Vif to determine their impact on the ability of Vif to degrade APOBEC3G. Vif-dependent degradation of APOBEC3G was measured by immunoblotting (66). Vif and APOBEC3G were transiently expressed in HeLa cells, separated by SDS-PAGE, and subjected to immunoblot analysis using antibodies to APOBEC3G, Vif, and tubulin (as a loading control). The APOBEC3G degradation data (Fig. 7a) indicate that the S165D and V166S Vif mutants were unable to efficiently degrade APOBEC3G and were comparable to the control lacking Vif. The APOBEC3G-degradation activity of the S165A mutant was comparable to that of wild type Vif. The ability of the Vif mutants to interact with APOBEC3G was tested by co-immunoprecipitation (*Materials and Methods*) (Fig. 7b–c). To prevent Vif-induced APOBEC3G degradation in this experiment, a dominant-negative form of Cul5 (Cul5ΔRbx) was co-transfected. The results demonstrate that all of the mutations weakened the Vif-APOBEC3G interaction irrespective of the functional phenotype. This suggests that mutations in Vif that affect interaction with APOBEC3G are not necessarily indicative for effects of Vif on APOBEC3G degradation. Nevertheless, the data in Fig. 6 and 7 reveal that the same residues involved in oligomerization are also important for APOBEC3G binding and degradation.

Discussion

This represents the first detailed hydrodynamic analysis of HIV-1 Vif oligomerization using AUC. A major finding of this study is that the PPLP motif is not essential for Vif oligomerization. Previous studies have suggested that the PPLP motif is essential for oligomerization (51, 52). These studies utilized an assay in which immobilized GST-Vif was used to pull down ^{35}S-labeled Vif. Our AUC studies are fundamentally different from these earlier studies because they are performed in solution. It is possible that the conformation of GST-Vif attached to the solid surface is different from the conformation in solution. Recently, AUC analysis of Vif(139–176), which contains the BC box and PPLP motif, revealed that this fragment of Vif is monomeric (46). Dynamic light scattering was used to examine the impact of the AALA mutation on Vif oligomerization (61). The authors found that this mutation reduced but did not abolish oligomerization. AUC revealed that the AALA mutation abolished monomeric Vif and stabilized higher-order oligomers (Fig. 6a). Mutation of the PPLP motif by the AALA may create a hydrophobic patch that stabilizes oligomeric forms of Vif. However, since the PPLP sequence is likely to impose very unique constraints on the conformation of Vif, indirect effects on oligomerization caused by the AALA mutation cannot be ruled out. Although the PPLP motif is clearly important for Vif function, our data and the studies mentioned support our assertion that the PPLP motif is not essential for oligomerization.

Our data suggest that the mechanism of oligomerization is more complex than previously thought. The HCCH motif appears to be involved in oligomerization. The c(*s*) profile of MBPVif(101–141) revealed the presence of oligomers (Fig. 5), and the weighted-average $s_{20,w}$ value for this construct was significantly greater than that for the monomer (Fig. 5, inset). It is important to emphasize that these studies were performed in the absence of zinc, which is known to alter the conformation of the HCCH motif (42, 67). Addition of zinc to MBP-Vif(101–176) altered its oligomeric properties, and this effect could be reversed by the

addition of EDTA (Supplemental Data, Fig. S2), further suggesting that Vif oligomerization is sensitive to the conformation of the HCCH motif. The BC box may also be involved in oligomerization. MBP-Vif(101–153) which includes the HCCH motif and BC box oligomerized to a greater extent than MBP-Vif(101–141). This can be seen by comparing the c(*s*) profiles for these constructs (Fig. 5) as well as their weighted-average $s_{20,w}$ values (Fig. 5, inset). Tween 20 (0.05% v/v) did not alter the c(*s*) profile for MBP-Vif(101–153) (data not shown), suggesting that oligomerization is mediated by specific protein-protein interactions. Even the subtle mutation of L145 to A in the BC box significantly altered the oligomeric properties of MBP-Vif(101–176) (Supplemental Data, Fig. S3). Thus, we favor a mechanism in which the HCCH motif, BC box, and PPLP motif interact to generate a conformation that promotes oligomerization.

Our studies highlight the biochemical and conformational properties of the PPLP peptide corresponding to Vif residues 155–176. This peptide lacked strong secondary structure. Interestingly, TFE induced alpha helical secondary structure in this peptide (Fig. 4) and promoted peptide oligomerization (inset to Fig. 4). In the absence of TFE, the peptide was monomeric even at a concentration as high as 1.8 mM. However, when the PPLP peptide was fused to the C terminus of MBP, which is normally monomeric, a significant amount of the fusion protein formed dimers (Fig. 3). Experiments using NMR (46) and hydrogen exchange mass spectrometry (50) suggest that the region containing the PPLP motif is highly dynamic. The fact the PPLP peptide was monomeric unless fused to MBP or MBP-Vif constructs (*e.g.* MBP-Vif(101–176)) suggests that this region of Vif may undergo induced folding to generate a conformation that promotes oligomerization. A similar induced-folding mechanism has been proposed to explain the interaction of the region containing the BC box and PPLP motif with elongin B/C (46, 50).

Residues immediately upstream from the PPLP motif (I^{154}TPKKIK^{160}) were most critical for oligomerization. This can seen by comparing the weighted-average $s_{20,w}$ values for MBP-Vif fragments 101–153, 101–160, and 101–165 (Fig. 5, inset). However, mutation of the PPLP motif (Fig. 6a) or residues immediately downstream from the PPLP motif (Fig. 6b) also perturbed the oligomeric properties of Vif. Mutation of V166 to S greatly affected the oligomeric properties of Vif, by destabilizing the monomeric form and stabilizing the dimeric form relative to wild type protein, which can be seen from the c(*s*) profiles in Fig. 6b. The oligomeric properties of Vif were sensitive to mutations at position 165. Replacement of serine at this position with either alanine or aspartate stabilized the monomeric form of Vif and destabilized higher-order oligomeric forms (Fig. 6b). S165 is highly conserved among HIV-1 Vif sequences and is thought to be targeted for phosphorylation by MAPK (68). Phosphorylation of S165 could provide a mechanism to modulate the conformation and oligomeric properties of Vif *in vivo*.

We tested the functional impact of the S165 and V166 mutations by determining the ability of the mutant Vif proteins to degrade APOBEC3G (Fig. 7a). The effect of the mutations can be rank ordered according to severity as V166S > S165D > S165A > wild-type Vif. The effect of these mutations on the oligomeric properties of Vif follows a similar trend (Fig. 6b). Interestingly, all the mutants were defective in their ability to interact with APOBEC3G (Fig. 7b–c), suggesting that the C terminus of HIV-1 Vif plays an important role in binding APOBEC3G. This effect could be direct or could be the result of misfolding caused by the mutations.

What we have learned is that oligomerization of HIV-1 Vif requires a region in the C terminus that encompasses the HCCH motif, BC box, and PPLP motif. The exact role of the PPLP motif in Vif function remains unclear, but we propose that its main role is to properly orient nearby residues that mediate protein-protein interactions. Vif is a dynamic protein and

this conformational complexity may be essential in order to mediate many different protein interactions like Cul5 binding, elongin B/C binding, Vif-Vif binding, and APOBEC3G binding. With regard to the oligomeric state of Vif, several oligomeric forms have been identified here and in other studies (44, 51, 61). Our results indicate that mutations which affect Vif oligomerization also affect the ability to bind and degrade APOBEC3G. One explanation is that a common surface in Vif mediates oligomerization and APOBEC3G binding. It is also possible that Vif oligomerization facilitates APOBEC3G binding. In the cell, APOBEC3G exists in a high molecular-mass form that is stabilized by RNA (69). Vif oligomers may be able to more avidly bind to the high molecular-mass form of APOBEC3G. On the other hand, a recent study found that Vif-elongin-B/C-Cul5 complexes contain monomeric Vif (44). Ultimately, the role of Vif is to exclude APOBEC3G from budding viral particles. Vif monomers may function to recruit the Cul5 ubiquitin ligase machinery and induce the degradation of APOBEC3G. Vif oligomers could stabilize high molecular-mass APOBEC3G complexes and prevent viral packaging of APOBEC3G by a degradation-independent pathway. Further studies are required to understand how Vif oligomerization affects its interactions with APOBEC3G as well as other binding partners.

Supplementary Material

Refer to Web version on PubMed Central for supplementary material.

Acknowledgments

The authors thank Sudipa Ghimire and Kalyan Giri for careful review of the manuscript.

This work was supported by the Edward Mallinckrodt Jr. Foundation (EM & ST), and the NIH Intramural Research Programs of the National Institute of Allergy and Infectious Diseases (KS & SK), and National Institute of Diabetes and Digestive and Kidney Diseases (RG).

References

1. Sheehy AM, Gaddis NC, Choi JD, Malim MH. Isolation of a human gene that inhibits HIV-1 infection and is suppressed by the viral Vif protein. Nature. 2002; 418:646–650. [PubMed: 12167863]
2. Bishop KN, Holmes RK, Sheehy AM, Davidson NO, Cho SJ, Malim MH. Cytidine deamination of retroviral DNA by diverse APOBEC proteins. Curr Biol. 2004; 14:1392–1396. [PubMed: 15296758]
3. Liddament MT, Brown WL, Schumacher AJ, Harris RS. APOBEC3F properties and hypermutation preferences indicate activity against HIV-1 in vivo. Curr Biol. 2004; 14:1385–1391. [PubMed: 15296757]
4. Wiegand HL, Doehle BP, Bogerd HP, Cullen BR. A second human antiretroviral factor, APOBEC3F, is suppressed by the HIV-1 and HIV-2 Vif proteins. Embo J. 2004; 23:2451–2458. [PubMed: 15152192]
5. Zheng YH, Irwin D, Kurosu T, Tokunaga K, Sata T, Peterlin BM. Human APOBEC3F is another host factor that blocks human immunodeficiency virus type 1 replication. J Virol. 2004; 78:6073–6076. [PubMed: 15141007]
6. Luo K, Liu B, Xiao Z, Yu Y, Yu X, Gorelick R, Yu XF. Amino-terminal region of the human immunodeficiency virus type 1 nucleocapsid is required for human APOBEC3G packaging. J Virol. 2004; 78:11841–11852. [PubMed: 15479826]
7. Cen S, Guo F, Niu M, Saadatmand J, Deflassieux J, Kleiman L. The interaction between HIV-1 Gag and APOBEC3G. J Biol Chem. 2004; 279:33177–33184. [PubMed: 15159405]
8. Alce TM, Popik W. APOBEC3G is incorporated into virus-like particles by a direct interaction with HIV-1 Gag nucleocapsid protein. J Biol Chem. 2004; 279:34083–34086. [PubMed: 15215254]

9. Douaisi M, Dussart S, Courcoul M, Bessou G, Vigne R, Decroly E. HIV-1 and MLV Gag proteins are sufficient to recruit APOBEC3G into virus-like particles. Biochem Biophys Res Commun. 2004; 321:566–573. [PubMed: 15358144]
10. Schafer A, Bogerd HP, Cullen BR. Specific packaging of APOBEC3G into HIV-1 virions is mediated by the nucleocapsid domain of the gag polyprotein precursor. Virology. 2004; 328:163–168. [PubMed: 15464836]
11. Svarovskaia ES, Xu H, Mbisa JL, Barr R, Gorelick RJ, Ono A, Freed EO, Hu WS, Pathak VK. Human apolipoprotein B mRNA-editing enzyme-catalytic polypeptide-like 3G (APOBEC3G) is incorporated into HIV-1 virions through interactions with viral and nonviral RNAs. J Biol Chem. 2004; 279:35822–35828. [PubMed: 15210704]
12. Zennou V, Perez-Caballero D, Gottlinger H, Bieniasz PD. APOBEC3G incorporation into human immunodeficiency virus type 1 particles. J Virol. 2004; 78:12058–12061. [PubMed: 15479846]
13. Khan MA, Kao S, Miyagi E, Takeuchi H, Goila-Gaur R, Opi S, Gipson CL, Parslow TG, Ly H, Strebel K. Viral RNA is required for the association of APOBEC3G with human immunodeficiency virus type 1 nucleoprotein complexes. J Virol. 2005; 79:5870–5874. [PubMed: 15827203]
14. Navarro F, Bollman B, Chen H, Konig R, Yu Q, Chiles K, Landau NR. Complementary function of the two catalytic domains of APOBEC3G. Virology. 2005; 333:374–386. [PubMed: 15721369]
15. Burnett A, Spearman P. APOBEC3G multimers are recruited to the plasma membrane for packaging into human immunodeficiency virus type 1 virus-like particles in an RNA-dependent process requiring the NC basic linker. J Virol. 2007; 81:5000–5013. [PubMed: 17344295]
16. Harris RS, Bishop KN, Sheehy AM, Craig HM, Petersen-Mahrt SK, Watt IN, Neuberger MS, Malim MH. DNA deamination mediates innate immunity to retroviral infection. Cell. 2003; 113:803–809. [PubMed: 12809610]
17. Lecossier D, Bouchonnet F, Clavel F, Hance AJ. Hypermutation of HIV-1 DNA in the absence of the Vif protein. Science. 2003; 300:1112. [PubMed: 12750511]
18. Mangeat B, Turelli P, Caron G, Friedli M, Perrin L, Trono D. Broad antiretroviral defence by human APOBEC3G through lethal editing of nascent reverse transcripts. Nature. 2003; 424:99–103. [PubMed: 12808466]
19. Mariani R, Chen D, Schrofelbauer B, Navarro F, Konig R, Bollman B, Munk C, Nymark-McMahon H, Landau NR. Species-specific exclusion of APOBEC3G from HIV-1 virions by Vif. Cell. 2003; 114:21–31. [PubMed: 12859895]
20. Zhang H, Yang B, Pomerantz RJ, Zhang C, Arunachalam SC, Gao L. The cytidine deaminase CEM15 induces hypermutation in newly synthesized HIV-1 DNA. Nature. 2003; 424:94–98. [PubMed: 12808465]
21. Yu X, Yu Y, Liu B, Luo K, Kong W, Mao P, Yu XF. Induction of APOBEC3G ubiquitination and degradation by an HIV-1 Vif-Cul5-SCF complex. Science. 2003; 302:1056–1060. [PubMed: 14564014]
22. Jager S, Kim DY, Hultquist JF, Shindo K, LaRue RS, Kwon E, Li M, Anderson BD, Yen L, Stanley D, Mahon C, Kane J, Franks-Skiba K, Cimermancic P, Burlingame A, Sali A, Craik CS, Harris RS, Gross JD, Krogan NJ. Vif hijacks CBF-beta to degrade APOBEC3G and promote HIV-1 infection. Nature. 2012; 481:371–375. [PubMed: 22190037]
23. Zhang W, Du J, Evans SL, Yu Y, Yu XF. T-cell differentiation factor CBF-beta regulates HIV-1 Vif-mediated evasion of host restriction. Nature. 2012; 481:376–379. [PubMed: 22190036]
24. Conticello SG, Harris RS, Neuberger MS. The Vif protein of HIV triggers degradation of the human antiretroviral DNA deaminase APOBEC3G. Curr Biol. 2003; 13:2009–2013. [PubMed: 14614829]
25. Kobayashi M, Takaori-Kondo A, Miyauchi Y, Iwai K, Uchiyama T. Ubiquitination of APOBEC3G by an HIV-1 Vif-Cullin5-Elongin B-Elongin C complex is essential for Vif function. J Biol Chem. 2005; 280:18573–18578. [PubMed: 15781449]
26. Marin M, Rose KM, Kozak SL, Kabat D. HIV-1 Vif protein binds the editing enzyme APOBEC3G and induces its degradation. Nat Med. 2003; 9:1398–1403. [PubMed: 14528301]

27. Mehle A, Strack B, Ancuta P, Zhang C, McPike M, Gabuzda D. Vif overcomes the innate antiviral activity of APOBEC3G by promoting its degradation in the ubiquitin-proteasome pathway. J Biol Chem. 2004; 279:7792–7798. [PubMed: 14672928]
28. Stopak K, de Noronha C, Yonemoto W, Greene WC. HIV-1 Vif blocks the antiviral activity of APOBEC3G by impairing both its translation and intracellular stability. Mol Cell. 2003; 12:591–601. [PubMed: 14527406]
29. Chen G, He Z, Wang T, Xu R, Yu XF. A patch of positively charged amino acids surrounding the human immunodeficiency virus type 1 Vif SLVx4Yx9Y motif influences its interaction with APOBEC3G. J Virol. 2009; 83:8674–8682. [PubMed: 19535450]
30. Dang Y, Davis RW, York IA, Zheng YH. Identification of 81LGxGxxIxW89 and 171EDRW174 domains from human immunodeficiency virus type 1 Vif that regulate APOBEC3G and APOBEC3F neutralizing activity. J Virol. 2010; 84:5741–5750. [PubMed: 20335268]
31. Dang Y, Wang X, Zhou T, York IA, Zheng YH. Identification of a novel WxSLVK motif in the N terminus of human immunodeficiency virus and simian immunodeficiency virus Vif that is critical for APOBEC3G and APOBEC3F neutralization. J Virol. 2009; 83:8544–8552. [PubMed: 19535447]
32. He Z, Zhang W, Chen G, Xu R, Yu XF. Characterization of conserved motifs in HIV-1 Vif required for APOBEC3G and APOBEC3F interaction. J Mol Biol. 2008; 381:1000–1011. [PubMed: 18619467]
33. Pery E, Rajendran KS, Brazier AJ, Gabuzda D. Regulation of APOBEC3 proteins by a novel YXXL motif in human immunodeficiency virus type 1 Vif and simian immunodeficiency virus SIVagm Vif. J Virol. 2009; 83:2374–2381. [PubMed: 19109396]
34. Russell RA, Pathak VK. Identification of two distinct human immunodeficiency virus type 1 Vif determinants critical for interactions with human APOBEC3G and APOBEC3F. J Virol. 2007; 81:8201–8210. [PubMed: 17522216]
35. Schrofelbauer B, Senger T, Manning G, Landau NR. Mutational alteration of human immunodeficiency virus type 1 Vif allows for functional interaction with nonhuman primate APOBEC3G. J Virol. 2006; 80:5984–5991. [PubMed: 16731937]
36. Mehle A, Goncalves J, Santa-Marta M, McPike M, Gabuzda D. Phosphorylation of a novel SOCS-box regulates assembly of the HIV-1 Vif-Cul5 complex that promotes APOBEC3G degradation. Genes Dev. 2004; 18:2861–2866. [PubMed: 15574592]
37. Yu Y, Xiao Z, Ehrlich ES, Yu X, Yu XF. Selective assembly of HIV-1 Vif-Cul5-ElonginB-ElonginC E3 ubiquitin ligase complex through a novel SOCS box and upstream cysteines. Genes Dev. 2004; 18:2867–2872. [PubMed: 15574593]
38. Luo K, Xiao Z, Ehrlich E, Yu Y, Liu B, Zheng S, Yu XF. Primate lentiviral virion infectivity factors are substrate receptors that assemble with cullin 5-E3 ligase through a HCCH motif to suppress APOBEC3G. Proc Natl Acad Sci U S A. 2005; 102:11444–11449. [PubMed: 16076960]
39. Mehle A, Thomas ER, Rajendran KS, Gabuzda D. A zinc-binding region in Vif binds Cul5 and determines cullin selection. J Biol Chem. 2006; 281:17259–17265. [PubMed: 16636053]
40. Xiao Z, Ehrlich E, Yu Y, Luo K, Wang T, Tian C, Yu XF. Assembly of HIV-1 Vif-Cul5 E3 ubiquitin ligase through a novel zinc-binding domain-stabilized hydrophobic interface in Vif. Virology. 2006; 349:290–299. [PubMed: 16530799]
41. Giri K, Scott RA, Maynard EL. Molecular Structure and Biochemical Properties of the HCCH-Zn^{2+} Site in HIV-1 Vif. Biochemistry. 2009; 48:7969–7978. [PubMed: 19588889]
42. Paul I, Cui J, Maynard EL. Zinc binding to the HCCH motif of HIV-1 virion infectivity factor induces a conformational change that mediates protein-protein interactions. Proc Natl Acad Sci U S A. 2006; 103:18475–18480. [PubMed: 17132731]
43. Stanley BJ, Ehrlich ES, Short L, Yu Y, Xiao Z, Yu XF, Xiong Y. Structural Insight into the HIV Vif SOCS Box and Its Role in Human E3 Ubiquitin Ligase Assembly. J Virol. 2008
44. Wolfe LS, Stanley BJ, Liu C, Eliason WK, Xiong Y. Dissection of HIV Vif interaction with the human E3 ubiquitin ligase. J Virol. 2010
45. Kamura T, Maenaka K, Kotoshiba S, Matsumoto M, Kohda D, Conaway RC, Conaway JW, Nakayama KI. VHL-box and SOCS-box domains determine binding specificity for Cul2-Rbx1 and Cul5-Rbx2 modules of ubiquitin ligases. Genes Dev. 2004; 18:3055–3065. [PubMed: 15601820]

46. Bergeron JR, Huthoff H, Veselkov DA, Beavil RL, Simpson PJ, Matthews SJ, Malim MH, Sanderson MR. The SOCS-box of HIV-1 Vif interacts with ElonginBC by induced-folding to recruit its Cul5-containing ubiquitin ligase complex. PLoS Pathog. 2010; 6:e1000925. [PubMed: 20532212]
47. Donahue JP, Vetter ML, Mukhtar NA, D'Aquila RT. The HIV-1 Vif PPLP motif is necessary for human APOBEC3G binding and degradation. Virology. 2008; 377:49–53. [PubMed: 18499212]
48. Walker RC Jr. Khan MA, Kao S, Goila-Gaur R, Miyagi E, Strebel K. Identification of dominant negative human immunodeficiency virus type 1 Vif mutants that interfere with the functional inactivation of APOBEC3G by virus-encoded Vif. J Virol. 2010; 84:5201–5211. [PubMed: 20219919]
49. Auclair JR, Green KM, Shandilya S, Evans JE, Somasundaran M, Schiffer CA. Mass spectrometry analysis of HIV-1 Vif reveals an increase in ordered structure upon oligomerization in regions necessary for viral infectivity. Proteins. 2007; 69:270–284. [PubMed: 17598142]
50. Marcsisin SR, Engen JR. Molecular insight into the conformational dynamics of the Elongin BC complex and its interaction with HIV-1 Vif. J Mol Biol. 2010; 402:892–904. [PubMed: 20728451]
51. Yang S, Sun Y, Zhang H. The multimerization of human immunodeficiency virus type I Vif protein: a requirement for Vif function in the viral life cycle. J Biol Chem. 2001; 276:4889–4893. [PubMed: 11071884]
52. Yang B, Gao L, Li L, Lu Z, Fan X, Patel CA, Pomerantz RJ, DuBois GC, Zhang H. Potent suppression of viral infectivity by the peptides that inhibit multimerization of human immunodeficiency virus type 1 (HIV-1) Vif proteins. J Biol Chem. 2003; 278:6596–6602. [PubMed: 12480936]
53. Miller JH, Presnyak V, Smith HC. The dimerization domain of HIV-1 viral infectivity factor Vif is required to block virion incorporation of APOBEC3G. Retrovirology. 2007; 4:81. [PubMed: 18036235]
54. Pace CN, Vajdos F, Fee L, Grimsley G, Gray T. How to measure and predict the molar absorption coefficient of a protein. Protein Sci. 1995; 4:2411–2423. [PubMed: 8563639]
55. Schuck P. Size-distribution analysis of macromolecules by sedimentation velocity ultracentrifugation and lamm equation modeling. Biophys J. 2000; 78:1606–1619. [PubMed: 10692345]
56. Cole JL, Lary JW, T PM, Laue TM. Analytical ultracentrifugation: sedimentation velocity and sedimentation equilibrium. Methods Cell Biol. 2008; 84:143–179. [PubMed: 17964931]
57. Provencher SW, Glockner J. Estimation of globular protein secondary structure from circular dichroism. Biochemistry. 1981; 20:33–37. [PubMed: 7470476]
58. Lees JG, Smith BR, Wien F, Miles AJ, Wallace BA. CDtool-an integrated software package for circular dichroism spectroscopic data processing, analysis, and archiving. Anal Biochem. 2004; 332:285–289. [PubMed: 15325297]
59. Lobley A, Whitmore L, Wallace BA. DICHROWEB: an interactive website for the analysis of protein secondary structure from circular dichroism spectra. Bioinformatics. 2002; 18:211–212. [PubMed: 11836237]
60. Whitmore L, Wallace BA. DICHROWEB, an online server for protein secondary structure analyses from circular dichroism spectroscopic data. Nucleic Acids Res. 2004; 32:W668–673. [PubMed: 15215473]
61. Bernacchi S, Mercenne G, Tournaire C, Marquet R, Paillart JC. Importance of the proline-rich multimerization domain on the oligomerization and nucleic acid binding properties of HIV-1 Vif. Nucleic Acids Res. 2011; 39:2404–2415. [PubMed: 21076154]
62. Henriet S, Richer D, Bernacchi S, Decroly E, Vigne R, Ehresmann B, Ehresmann C, Paillart JC, Marquet R. Cooperative and specific binding of Vif to the 5' region of HIV-1 genomic RNA. J Mol Biol. 2005; 354:55–72. [PubMed: 16236319]
63. Bernacchi S, Henriet S, Dumas P, Paillart JC, Marquet R. RNA and DNA binding properties of HIV-1 Vif protein: a fluorescence study. J Biol Chem. 2007; 282:26361–26368. [PubMed: 17609216]

64. Zhao H, Brown PH, Balbo A, Fernandez-Alonso Mdel C, Polishchuck N, Chaudhry C, Mayer ML, Ghirlando R, Schuck P. Accounting for solvent signal offsets in the analysis of interferometric sedimentation velocity data. Macromol Biosci. 2010; 10:736–745. [PubMed: 20480511]

65. Buck M. Trifluoroethanol and colleagues: cosolvents come of age. Recent studies with peptides and proteins. Q Rev Biophys. 1998; 31:297–355. [PubMed: 10384688]

66. Kao S, Goila-Gaur R, Miyagi E, Khan MA, Opi S, Takeuchi H, Strebel K. Production of infectious virus and degradation of APOBEC3G are separable functional properties of human immunodeficiency virus type 1 Vif. Virology. 2007; 369:329–339. [PubMed: 17825339]

67. Giri K, Maynard EL. Conformational analysis of a peptide approximating the HCCH motif in HIV-1 Vif. Peptide Science. 2009; 92:417–425. [PubMed: 19382167]

68. Yang X, Goncalves J, Gabuzda D. Phosphorylation of Vif and its role in HIV-1 replication. J Biol Chem. 1996; 271:10121–10129. [PubMed: 8626571]

69. Chiu YL, Soros VB, Kreisberg JF, Stopak K, Yonemoto W, Greene WC. Cellular APOBEC3G restricts HIV-1 infection in resting CD4+ T cells. Nature. 2005; 435:108–114. [PubMed: 15829920]

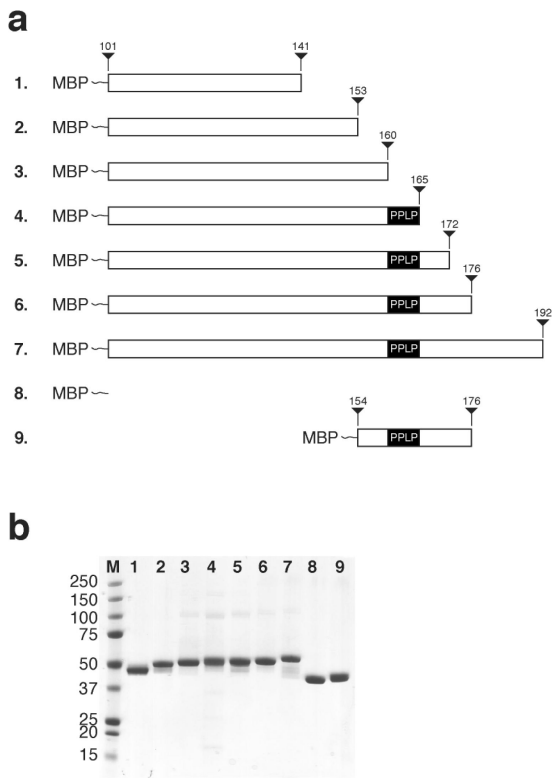

Figure 1.

(**a**) Constructs used in this study. **(b)** SDS-PAGE of protein constructs. Purified proteins were boiled in reducing SDS sample buffer, separated on a 4–12% gel, and visualized by staining with Colloidal Blue. Molecular weight standards are shown in kDa.

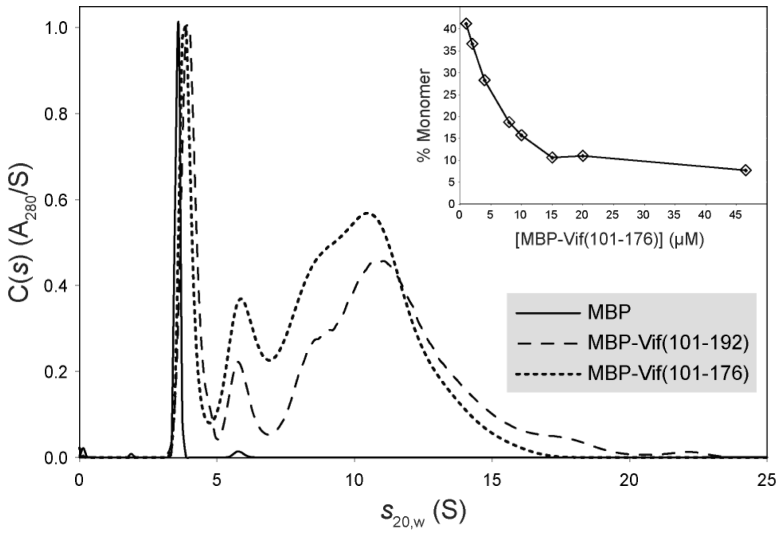

Figure 2.

Sedimentation velocity analytical ultracentrifugation of MBP, MBP-Vif(101–192) and MBP-Vif(101–176). Proteins were concentrated to 10 μM. AUC data were analyzed as a continuous c(*s*) distribution in SEDFIT as described in *Materials and Methods.* To compare the extent of oligomerization for each protein construct, the c(*s*) plots were normalized to the area under the monomer peak. ***Inset:*** Analysis of the reversibility of MBP-Vif(101–176) oligomerization. Protein samples were prepared by serial dilution of a 46.5 μM stock solution. AUC data were analyzed as described in *Materials and Methods.* Percent monomeric Vif is plotted as a function of protein loading concentration.

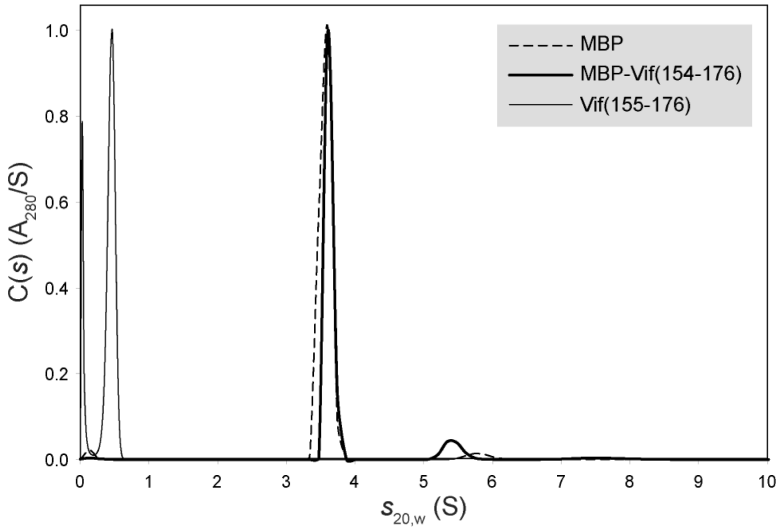

Figure 3.

Sedimentation behavior of a Vif-PPLP peptide, free in solution or fused to maltose binding protein. Sedimentation velocity AUC data were analyzed as a continuous c(*s*) distribution of sedimenting species. C(*s*) profiles are shown for MBP (10 μM), MBP-Vif(154–176) (12 μM), and for a synthetic PPLP peptide corresponding to Vif residues 155–176 (1.8 mM).

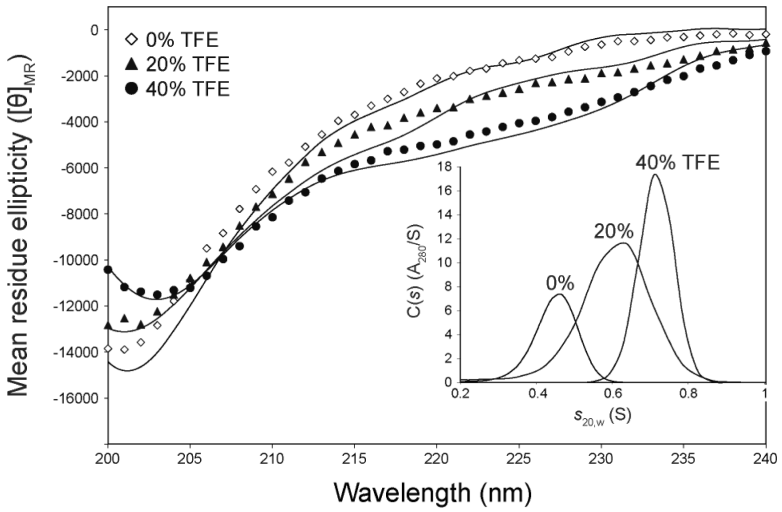

Figure 4.

Trifluoroethanol-induced changes in the secondary structure and oligomeric properties of the Vif(155–176) peptide. Far-UV circular dichroism spectra of Vif(155–176) (48 μM final concentration) prepared in buffer containing 0%, 20%, or 40% (v/v) TFE. ***Inset:*** C(*s*) profiles for Vif(155–176) (140 μM final concentration) in the presence of 0%, 20%, or 40% TFE.

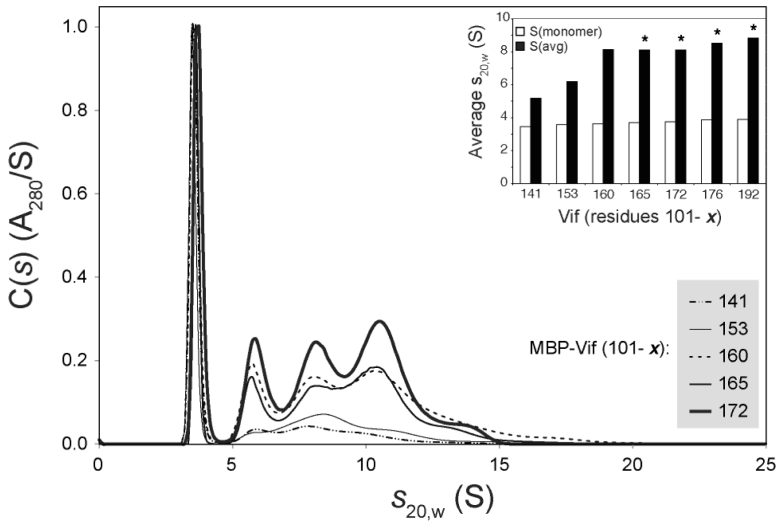

Figure 5.

Oligomeric properties of Vif truncation mutants. Sedimentation velocity AUC experiments were conducted with MBP-Vif(101- *x*) fragments where *x* = 141, 153, 160, 165, or 172. Proteins were purified as described and concentrated to 10 μM. AUC data were analyzed as described. For comparison, the c(*s*) profiles were normalized according to the area under the monomer peak. ***Inset:*** Weighted-average $s_{20,w}$ values for MBP-Vif(101- *x*) constructs. Sedimentation velocity AUC analyses were performed using an equivalent concentration (10 μM final) for all protein constructs. Weighted-average $s_{20,w}$ values (filled bars) were calculated by integrating the c(*s*) profiles from 2 S to 20 S. Empty bars represent the $s_{20,w}$ value for the monomer species. Bars corresponding to constructs that contain the PPLP motif are marked with an asterisk.

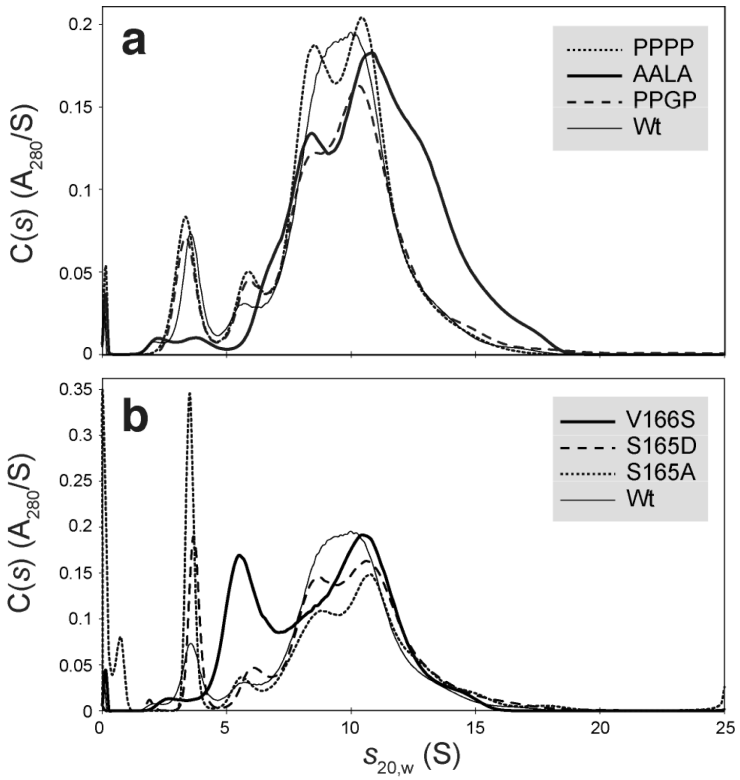

Figure 6.

Oligomeric properties of Vif mutants. **(a)** Mutations in the PPLP motif (AALA, PPGP, and PPPP) were created in the MBP-Vif(101–176) construct and purified proteins were concentrated to 30 μM. Proteins were analyzed by sedimentation velocity AUC. **(b)** Point mutations, S165A, S165D, and V166S, were created in the MBP-Vif(101–176) construct and purified proteins were concentrated to 30 μM. Sedimentation velocity AUC data were analyzed as described in *Materials and Methods*.

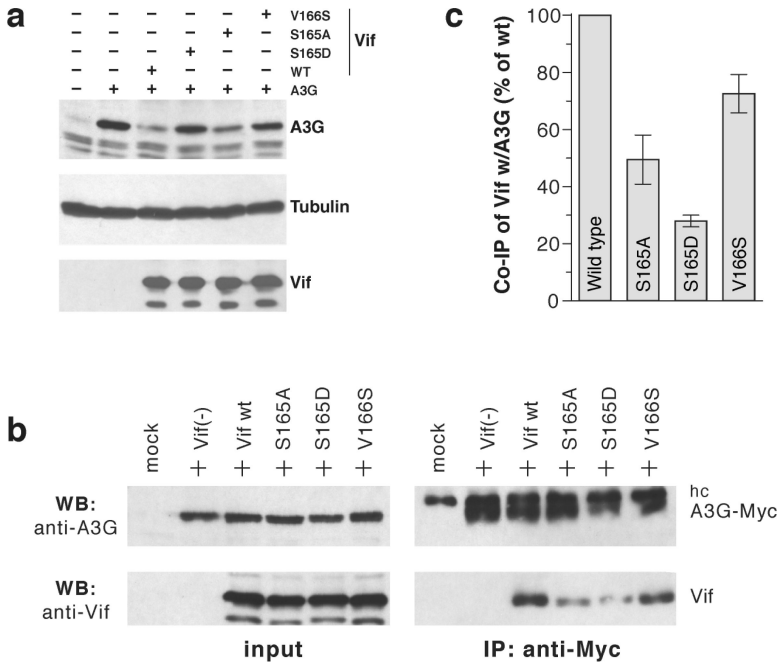

Figure 7.

Functional analysis of S165 and V166 mutants of Vif. **(a)** Vif-induced degradation of APOBEC3G. HeLa cells transiently expressing Vif and APOBEC3G were harvested and probed using antibodies to APOBEC3G or Vif. **(b)** Co-immunoprecipitation of Vif and APOBEC3G. HeLa cells were transfected with vectors encoding Vif, APOBEC3G-Myc, and Cul5ΔRbx. Cul5ΔRbx was included to prohibit Vif-induced degradation of A3G in this experiment (21). Anti-Myc immunoprecipitates were separated by SDS-PAGE and probed with antibodies to Vif and Myc (right). Total cell extracts served as input control and were used to correct for fluctuations in Vif expression levels (left). **(c)** Results from three independent experiments were quantified. Amount of co-precipitated wt Vif is defined as 100% and the amount of co-precipitated mutant Vif protein is expressed as a percentage of wt Vif.